Stem Cell Research (2014) 12, 452–466

Available online at www.sciencedirect.com

ScienceDirect

www.elsevier.com/locate/scr

Role of STIM1 in survival and neural differentiation of mouse embryonic stem cells independent of Orai1-mediated Ca^{2+} entry☆

Baixia Hao, Yingying Lu, Qian Wang, Wenjing Guo, King-Ho Cheung, Jianbo Yue*

Department of Physiology, University of Hong Kong, Hong Kong, China

Received 16 August 2013; received in revised form 10 December 2013; accepted 17 December 2013
Available online 27 December 2013

Abstract Store-operated Ca^{2+} entry (SOCE) is an important Ca^{2+} influx pathway in non-excitable cells. STIM1, an ER Ca^{2+} sensor, and Orai1, a plasma membrane Ca^{2+} selective channel, are the two essential components of the Ca^{2+} release activated channel (CRAC) responsible for SOCE activity. Here we explored the role of STIM1 and Orai1 in neural differentiation of mouse embryonic stem (ES) cells. We found that STIM1 and Orai1 were expressed and functionally active in ES cells, and expressions of STIM1 and Orai1 were dynamically regulated during neural differentiation of mouse ES cells. STIM1 knockdown inhibited the differentiation of mouse ES cells into neural progenitors, neurons, and astrocytes. In addition, STIM1 knockdown caused severe cell death and markedly suppressed the proliferation of neural progenitors. Surprisingly, Orai1 knockdown had little effect on neural differentiation of mouse ES cells, but the neurons derived from Orai1 knockdown ES cells, like those from STIM1 knockdown cells, had defective SOCE. Taken together, our data indicate that STIM1 is involved in both early neural differentiation of ES cells and survival of early differentiated ES cells independent of Orai1-mediated SOCE.

Introduction

The mechanism of neurogenesis is one of the most daunting questions in biology, largely due to the complexity of the processes (Gaspard and Vanderhaeghen, 2010). Because of their unique self-renewal and pluripotent properties, embryonic stem (ES) cells have recently become a promising resource that complements in vivo approaches for the study of neural differentiation. ES cells can be expanded in culture indefinitely while retaining the capacity to produce seemingly every type of fetal and adult cell (Evans and Kaufman, 1981). This property also endows ES cells to be promising candidates in regenerative medicine (Abdelwahid et al., 2011; Kim et al., 2002; Chhabra and Brayman, 2013; Lippmann et al., 2012). For

Abbreviations: DIC, Differential interference contrast; EB, Embryoid body; ES, Embryonic stem; LIF, Leukemia inhibitory factor; RA, Retinoic acid; SOCE, Store-operated Ca^{2+} entry; TRPC, Transient receptor potential channel; VGCC, Voltage gated Ca^{2+} channel.

* Corresponding author.
E-mail address: jbyue@me.com (J. Yue).

1873-5061/$ - see front matter © 2013 The Authors. Published by Elsevier B.V. All rights reserved.
http://dx.doi.org/10.1016/j.scr.2013.12.005

example, functional neurons differentiated from ES cells have been used to treat various neurodegenerative diseases, e.g. Parkinson's disease (Tian et al., 2012; Lindvall, 2012; Cajanek et al., 2009; Kriks et al., 2011). Yet, target neural differentiation of ES cells is still a challenge. Originally, only a small portion of neural population was generated from embryoid body (EB) formation or a suspension culture of single ES cell (Tropepe et al., 2001; Wiles and Johansson, 1999). Later, a higher efficiency of neural differentiation from ES cells was achieved by treatment of EB with retinoic acid (RA) or co-culture with PA6 stromal cells (Bain et al., 1995; Kawasaki et al., 2000). However, EB derived neurons were highly heterogeneous and were always contaminated with other cell types. In addition, the enhanced effects of RA and PA6 stromal cells on ES differentiation were not specific and mechanistically undefined. More recently, a monolayer adherent culture of mouse ES cells was utilized to more efficiently differentiate ES cells into neural lineage in a defined medium (Ying and Smith, 2003; Ying et al., 2003). Yet, still ~40% of cells couldn't enter a neural fate by this simple method. Thus, to achieve a high efficiency of directed neural differentiation of ES cells that are suitable for cell replacement therapy, it is important to identify novel signaling molecules or events that could play a role in the commitment of the neural lineages. We have been studying the role of Ca^{2+} signaling in the context of neural differentiation of ES cells.

Ca^{2+} signaling plays essential roles in a wide variety of cellular processes, from gene transcription to cell proliferation and differentiation (Berridge et al., 2003; Clapham, 2007). Ca^{2+} mobilization is coordinated by different Ca^{2+} channels and pumps that span the plasma membrane or the organelle membrane. Store-operated Ca^{2+} entry (SOCE) is an important Ca^{2+} influx pathway, especially in non-excitable cells, such as T lymphocytes (Parekh and Putney, 2005). STIM1 and Orai1 are the two essential components of SOCE, serving as ER Ca^{2+} sensor and pore forming subunit, respectively (Zhang et al., 2005; Vig et al., 2006a). Generally, Ca^{2+} release from the ER empties the ER Ca^{2+} pool and initiates Ca^{2+} dissociation from the EF hand domain of STIM1. Subsequently, oligomerization of STIM1 occurs, followed by STIM1 translocation to the ER-PM junction, where it interacts with and activates Orai1 to trigger Ca^{2+} influx. This phenomenon is also termed as Ca^{2+} release activated Ca^{2+} entry (Wang et al., 2010a). In addition, STIM1 can sense various cellular stresses, such as hypoxia, acidification, and temperature, to modulate the activity of SOCE (Hawkins et al., 2010; Mancarella et al., 2011; Xiao et al., 2011; S. Li et al., 2012). Other than activating the Orai1 channel, STIM1 was found to regulate transient receptor potential channels (TRPCs) and voltage gated Ca^{2+} channels (VGCCs) by direct interaction with these channel proteins (Kim et al., 2009; Park et al., 2010; Wang et al., 2010b). Unlike other channels, Orai1 is characterized by its high selectivity to Ca^{2+} (Vig et al., 2006b).

STIM1 and Orai1 mediated SOCE has been implicated in a wide range of cellular functions. The loss of functional STIM1 and Orai1 leads to autoimmunity and immunodeficiency in human patients (Feske et al., 2006; Picard et al., 2009). Likewise, STIM1 and Orai1 knockout mice show defective immune response (Oh-Hora et al., 2008; Gwack et al., 2008). In addition, STIM1 and Orai1 signaling is required for the contractility of skeletal muscle (Stiber et al., 2008), development of pathological cardiac hypertrophy (Hulot et al., 2011), growth of vascular smooth muscle (Zhang et al., 2011), tumor development (Feng et al., 2010), and thrombin stimulation of platelets (Braun et al., 2009).

Since their discovery, STIM1 and Orai1 mediated SOCE in various types of neurons and astrocytes has been documented (Li et al., 2009; Gruszczynska-Biegala et al., 2011; Koss et al., 2013; Moreno et al., 2012). Moreover, SOCE has been shown to play roles in a variety of neuronal activity, e.g. controlling *Drosophila* flight (Venkiteswaran and Hasan, 2009), turning of growth cones in response to extracellular stimuli (Mitchell et al., 2012), regulating neuronal excitability (Gemes et al., 2011), and modulating neuronal network activity (Steinbeck et al., 2011). Yet, the role of SOCE in early neural development remains to be determined. Here we examined the roles of STIM1 and Orai1 during neural differentiation of mouse ES cells and found that STIM1, not Orail1, is involved in early neural differentiation of ES cells and survival of differentiated ES cells.

Results

Characterization of SOCE in mouse ES cells

To examine the presence of functional SOCE in mouse ES cells, Fura-2 loaded ES cells were first treated with thapsigargin (TG), a specific SERCA inhibitor, to deplete the ER Ca^{2+} pools in the absence of extracellular Ca^{2+}. After cytosolic Ca^{2+} returned to basal levels, extra Ca^{2+} was added to the medium to trigger Ca^{2+} influx, and this Ca^{2+} influx was markedly inhibited by the Orai1 channel blockers, Gd^{3+} or 2-APB (Figs. 1A and B). These data indicate that SOCE occurs normally in mouse ES cells.

Upon the withdrawal of self-renewal stimuli, mouse ES cells spontaneously differentiate into neural progenitors in adherent monoculture (Ying and Smith, 2003; Ying et al., 2003). We, thus, examined the expression pattern of STIM1 and Orai1 during this process by quantitative RT-PCR. As shown in Figs. 1C and D, the mRNA expressions of STIM1 (Fig. 1C) and Orai1 (Fig. 1D) were initially markedly increased after 3 days of neural differentiation, yet by day 6, their expression all went down, thereafter their levels gradually rebounded during the late stages of neuronal genesis of ES cells. Interestingly, the mRNA expressions of STIM1 and Orai1 were also markedly increased in heterogeneously differentiated EBs, generated by aggregating ES cells in suspension (Figs. S1A and S1B). Notably, expression of Orai1 was initially decreased (day 3) but was later significantly increased (day 8) during EB formation (Fig. S1B). These data suggest that STIM1 or Orail might play a role in general, including neural, differentiation of mouse ES cells.

STIM1 and Orai1 knockdown in mouse ES cells

Subsequently, we knocked down the expression of STIM1 or Orai1 in three mouse ES cell lines, including D3, R1, and 46C Sox1-GFP, by infecting cells with lentiviruses carrying expression cassettes that encode short hairpin RNAs (shRNA) against mouse STIM1 or Orai1, respectively (Table S1 and Fig. S2). STIM1 or Orai1 were efficiently knocked down by two distinct shRNAs (Figs. 2A, B, and S2). Not surprisingly, the activity of SOCE was markedly suppressed in STIM1 or Orai1 knockdown cells compared to that in control cells, whereas STIM1 or Orai1 knockdown had no effects on ER Ca^{2+} levels, as indicated by the similar TG-induced Ca^{2+}

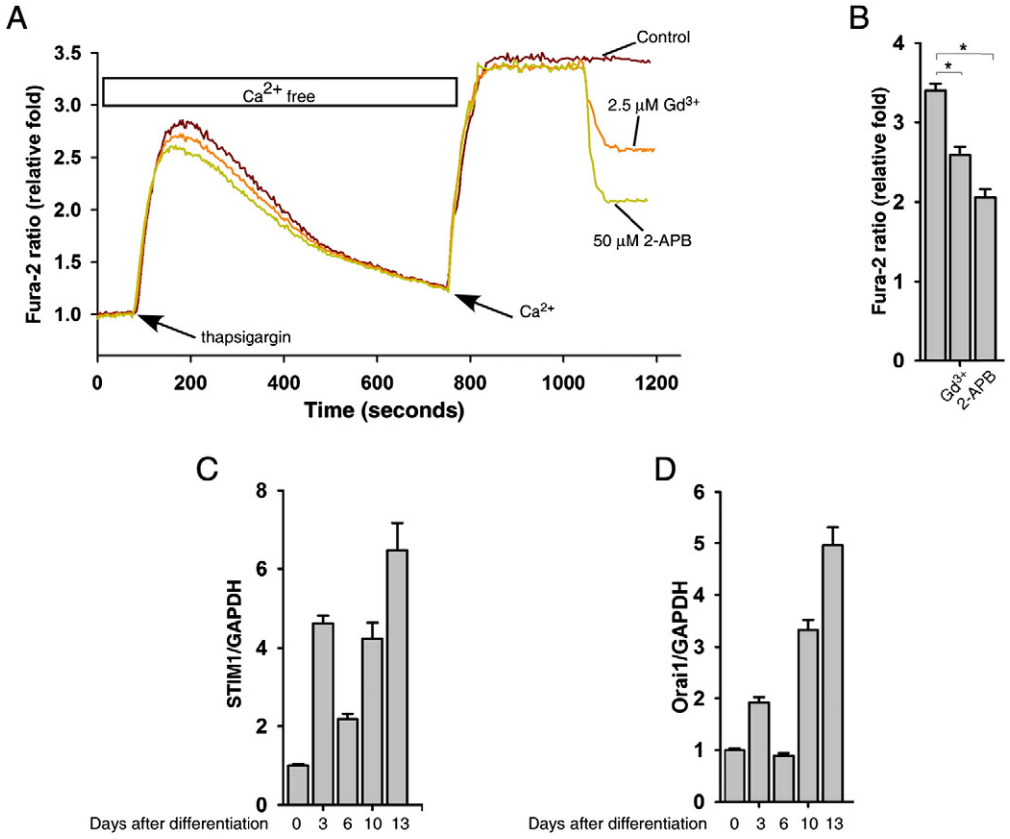

Figure 1 Characterization of SOCE in mouse ES cells. (A) Thapsigargin (1 μM) induced-Ca^{2+} influx was inhibited by Gd^{3+} or 2-APB treatment in Fura-2 loaded mouse ES cells. (B) Quantifications of the peak of Ca^{2+} influx in (A) were expressed as mean ± S.E., n = 30–50 cells, $^{*}p < 0.05$. (C) and (D) expression of STIM1 (C) and Orai1 (D) in the neural differentiation of D3 ES cells was determined by quantitative real-time RT-PCR.

changes in these cells (Fig. 2C). Compared to scramble shRNA infected cells, STIM1 knockdown or Orai1 knockdown ES cells exhibited no difference in alkaline phosphatase activity (Fig. 3A) and the expression of Oct4 (Fig. 3B) and Nanog (Fig. 3C) either in the presence or absence of LIF. In addition, STIM1 knockdown or Orai1 knockdown ES cells proliferated normally, compared to the control cells, in the presence or absence of LIF (Figs. 3D and E), and their cell cycle profiles were similar to that of control cells as well (Fig. 3F). These data suggest that neither STIM1 nor Orai1 plays an important role in the self-renewal of mouse ES cells.

Involvement of STIM1 in early neural differentiation of mouse ES cells

We next explored the effect of STIM1 knockdown on early neural differentiation of mouse ES cells. STIM1 knockdown and scramble shRNA expressing Sox1-GFP ES cell lines, in which GFP is targeted into the sox1 locus (Ying and Smith, 2003; Ying et al., 2003), were induced to differentiate into neural lineages following the monolayer culture protocol. After 4 days of neural differentiation, we found that fewer STIM1 knockdown cells became Sox1-GFP positive compared to control cells (Fig. 4A). FACS analyses were then performed to quantitate Sox1-GFP positive cells and confirmed that fewer Sox1-GFP positive neural progenitors appeared in STIM1 knockdown cells than control cells during early neural differentiation, particularly on day 4 (Fig. 4B). Western blot analysis also showed that the expression of Sox1 was markedly decreased in STIM1 knockdown cells than control cells (Fig. 4C). Similarly, STIM1 knockdown inhibited the expression of Nestin, another neural progenitor marker, during neural differentiation of mouse ES cells (Fig. S3). These data indicate that STIM1 is involved in the early neural differentiation of mouse ES cells.

STIM1 knockdown caused severe cell death during early neural differentiation of mouse ES cells

During neural differentiation of mouse ES cells initiated by monolayer culture in a defined medium without serum, differentiated cells undergo dramatic cell death (20%–30%) about 4–5 days after differentiation and a majority of the surviving cells adopt a neural fate (Ying and Smith, 2003; Ying et al., 2003). Strikingly, few of the STIM1 knockdown cells survived after day 4 of differentiation compared to control cells (Fig. 5A). We then performed the cell cycle analysis of the propidium iodide (PI) stained cells to assess apoptotic cells in differentiated cells (Riccardi and Nicoletti, 2006). As shown in Fig. 5B, more apoptotic cells existed in STIM1 knockdown cells than control cells, as indicated by the broad hypodiploid (sub-G1) peak. In addition, more STIM1 knockdown cells were in G_0/G_1, and fewer of them were in

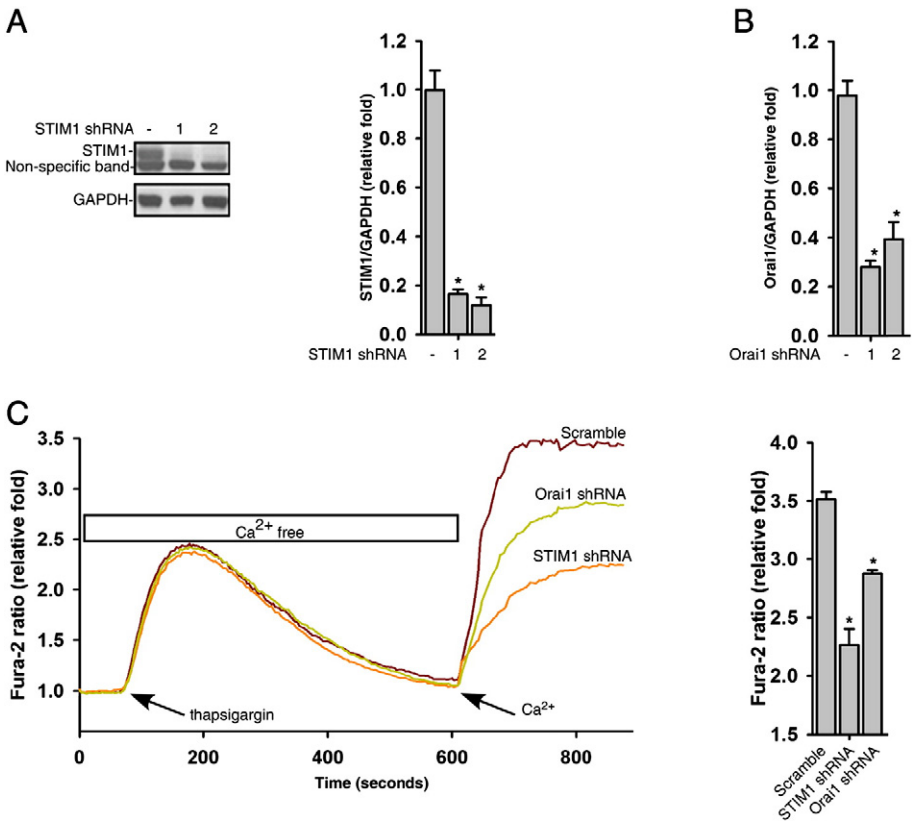

Figure 2 STIM1 and Orai1 knockdown in mouse ES cells. (A) STIM1 knockdown by two distinctive shRNAs in ES cells was verified by western blot analysis. (B) Orai1 knockdown by two distinctive shRNAs in ES cells was verified by qRT-PCR analysis. (C) STIM1 and Orai1 knockdown compromised thapsigargin-triggered SOCE in ES cells. Quantifications of the peak of Ca^{2+} influx were expressed as mean ± S.E., n = 30–50 cells, $^*p < 0.05$.

the S phase, compared to control cells (Fig. 5B), suggesting that STIM1 knockdown also inhibits proliferation of differentiated cells. A TUNEL assay further showed that more STIM1 knockdown cells underwent programmed cell death during differentiation (Fig. 5C). Interestingly, we also found that the STIM1 protein level was highest on day 4 after neural differentiation (Fig. 5D), which is consistent with its mRNA expression pattern shown by qRT-PCR (Fig. 1C), hinting that high expression level of STIM1 on day 4 after neural differentiation might be essential for cell survival. Since non-neural cells could not survive in the conditioned medium without FBS in the said monolayer adherent culture (Ying and Smith, 2003; Ying et al., 2003), it is possible that several cell death found in STIM1 knockdown cells is because of fewer neural cells differentiated from STIM1 knockdown ES cells. Nevertheless, these data suggest that STIM1 is involved in the survival of differentiated ES cells. Whether STIM1-mediated SOCE is involved in this process and whether STIM1 knockdown regulates the viability of neural progenitors remain to be determined.

Involvement of STIM1 in the late differentiation of mouse ES cells into neurons and astrocytes

Terminal differentiation of ES cell derived neural progenitors into neurons or astrocytes can be promoted by replating the neural progenitor cells onto poly-L-lysine-laminin coated plates after 6 days of monolayer culture (Ying and Smith, 2003; Ying et al., 2003). Consistently, STIM1 knockdown markedly inhibited expression of Tuj1, a neuronal marker, during the late stage of neural differentiation of ES cells (Fig. 6A). Likewise, immunostaining analyses found that fewer Tuj1 positive cells appeared in late STIM1 knockdown differentiated cells compared to control cells (Figs. 6B and C). In addition, western blot analysis showed the STIM1 knockdown markedly suppressed the expression of GFAP, an astrocyte marker, during the late neural differentiation of ES cells (Fig. 6D). Interestingly, the cell viability of the terminally differentiated neural cells was not affected by STIM1 knockdown (Fig. S4). Taken together, these data suggest that STIM1 is involved in the terminal differentiation of mouse ES cells into neurons and astrocytes. Yet, it remains possible that the decreased Tuj1 and GFAP in late neuronal differentiation of STIM1 knockdown cells is due to less Sox1 positive cells to begin with.

Orai1 knockdown failed to affect the neural differentiation of mouse ES cells

Likewise, Orai1 knockdown Sox1-GFP ES cells were induced to differentiate into neural lineages following the monolayer culture protocol. Unexpectedly, FACS analysis showed that a similar portion of Sox1-GFP positive cells existed in Orai1 knockdown or control differentiated cells (Figs. 7A and B). Similarly, Orai1 knockdown did not affect the expression of

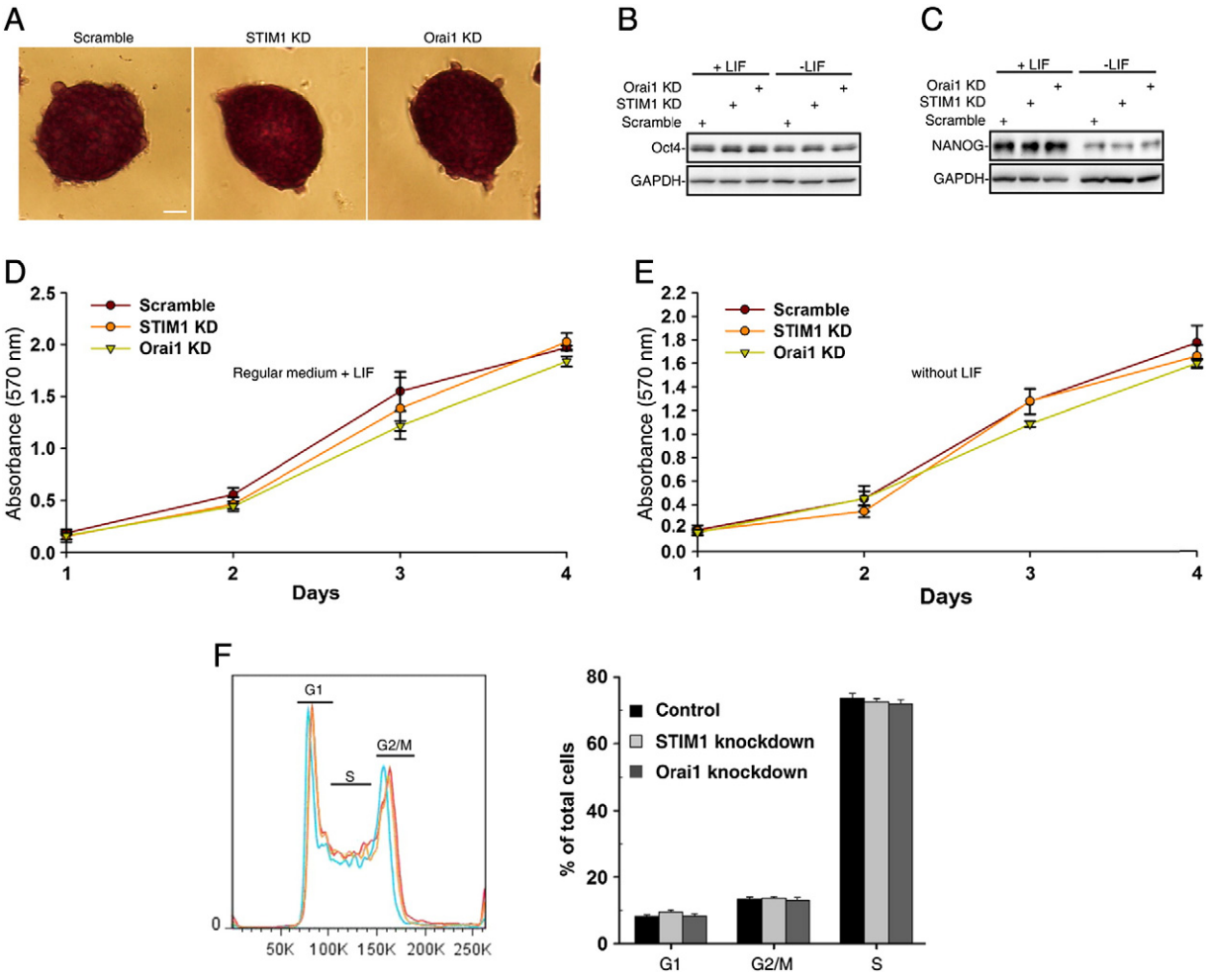

Figure 3 STIM1 or Orai1 knockdown did not affect the self-renewal and pluripotency of mouse ES cells. (A) Alkaline phosphatase (AP) staining of control, STIM1 knockdown, and Orai1 knockdown ES cells (Scale bar = 50 μm). (B) and (C) expression of Oct4 (B) and Nanog (C) in control, STIM1 knockdown, and Orai1 knockdown ES cells in the presence or absence of LIF were determined by western blot analyses. (D) and (E) MTT assay of control, STIM1 knockdown, and Orai1 knockdown ES cells in the presence (D) or absence (E) of LIF. (F) FACS analyses of DNA contents (PI staining) in control, STIM1 knockdown, and Orai1 knockdown ES cells. Quantifications of the percentage of cells in each phase were expressed as mean ± S.E., n = 3.

two neural progenitor markers, including Sox1 and Nestin, as assessed by western blot and qRT PCR analyses (Figs. 7C, D, and F). In addition, Orai1 knockdown had no effects on the expression of Tuj1 and GFAP during the late neural differentiation of ES cells (Figs. 7E–G). In summary, these data indicate that Orai1, in contrast to STIM1, is not involved in neural differentiation of mouse ES cells.

Ca^{2+} handling in STIM1 knockdown or Orai1 knockdown ES cell derived neurons

It is possible that the Ca^{2+} handling in STIM1 knockdown cells differs from that of Orai1 knockdown cells, thereby resulting in different neural differentiation phenotypes in respective knockdown ES cells. We thus first assessed the SOCE in both wildtype and STIM1 knockdown ES cell derived neurons. As shown in Fig. 8A, SOCE was functionally active in wildtype ES cell derived neurons, but STIM1 knockdown indeed compromised the SOCE in neurons, which was similar to that in STIM1 knockdown ES cells (Fig. 2C). Since it has been shown previously that STIM1 activation by ER Ca^{2+} store depletion strongly suppresses the activity of voltage-operated calcium channels (VGCCs) (Wang et al., 2010b), we also checked whether the activity of VGCCs is affected by STIM1 knockdown. In excitable cells, KCl can be applied to depolarize membrane potential, thereby activating VGCCs. As shown in Fig. 8B, KCl indeed triggered voltage gated Ca^{2+} entry in neurons derived from wildtype ES cells, and this was markedly increased in neurons differentiated from STIM1 knockdown ES cells. Similar data were also observed in STIM1 knockdown undifferentiated ES cells (Fig. S5). These data suggest that STIM1 knockdown compromises SOCE but enhances Ca^{2+} entry via VGCCs in ES cell derived neurons.

We next examined whether SOCE is also compromised in Orai1 knockdown ES cell derived neurons. As expected, Orai1 knockdown also inhibited SOCE in ES cell-derived neurons (Fig. 8C). Yet, KCl triggered similar levels of cytosolic Ca^{2+} increase in both control and Orai1 knockdown ES cell derived neurons (Fig. 8D), suggesting that Orai1 is not

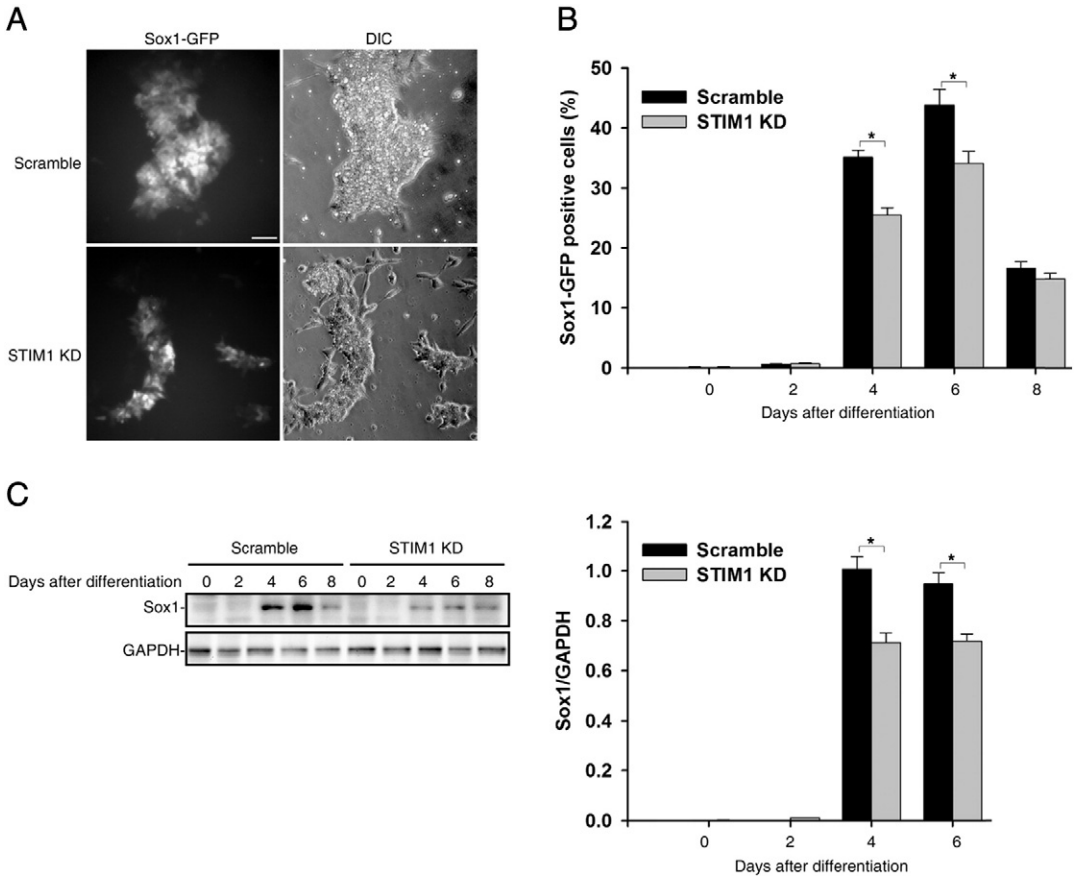

Figure 4 STIM1 knockdown inhibited neural lineage entry of 46C Sox1-GFP mouse ES cells. (A) GFP cell imaging and bright field of the Sox1-GFP positive cells in both control and STIM1 knockdown ES cells on day 4 after neural differentiation (Scale bar = 50 μm). (B) Quantification of FACS analyses of Sox1-GFP positive neural progenitors in viable control and STIM1 knockdown ES cells harvested at the indicated time point during neural differentiation. Data are expressed as mean ± S.E., n = 3, $*p < 0.05$. (C) Cell lysates were harvested at indicated time points during neural differentiation in both control and STIM1 knockdown cells, and analyzed for expression of Sox1 by western blot analyses.

involved in VGCCs regulation as reported previously (Park et al., 2010; Wang et al., 2010b). Taken together, these data suggest that STIM1 is involved in neural differentiation of ES cells independent of Orai1-mediated SOCE.

Discussion

Here we studied the role of two essential components of SOCE, STIM1 and Orai1, in the process of neural differentiation of mouse ES cells. We found that STIM1 knockdown, not Orai1 knockdown, markedly inhibited the early and late neural differentiation of mouse ES cells (Figs. 4–7). Interestingly, Ca^{2+} entry through VGCCs in neurons derived from STIM1 knockdown, not Orai1 knockdown, ES cells was enhanced. On the other hand, SOCE in both STIM1 knockdown and Orai1 knockdown neurons was compromised (Fig. 8). Moreover, STIM1 knockdown, not Orai1 knockdown, induced severe cell loss and suppressed the proliferation of neural progenitors derived from mouse ES cells (Fig. 5). Yet, STIM1 knockdown or Orai1 knockdown had no effect on the proliferation and survival of undifferentiated ES cells (Fig. 3). These results indicate that STIM1 is involved in both early neural differentiation of ES cells and survival of differentiated ES cells independent of Orai1-mediated SOCE.

Oct4 and Nanog are essential transcription factors that maintain the self-renewal and pluripotency of ES cells (Loh et al., 2006; Nichols et al., 1998; Chambers et al., 2003). Here we found that expressions of Oct4 and Nanog in STIM1 knockdown or Orai1 knockdown cells were similar to those in control cells (Figs. 3B and C). The activity of alkaline phosphatase, another indicator for pluripotency, also wasn't affected by STIM1 or Orai1 knockdown (Fig. 3A). In addition, STIM1 knockdown or Orai1 knockdown had little effect on cell proliferation and cell cycle profile of ES cells (Figs. 3D–F). These data indicate that STIM1 and Orai1 mediated SOCE signaling pathway is not required for the stemness of mouse ES cells. Along this line, it has been previously shown that the manipulation of other Ca^{2+} signaling pathways, including IP_3/IP_3R, cADPR/CD38 and NAADP/TPC2 Ca^{2+} signaling pathways, also exhibited no effect on the self-renewal and pluripotency of mouse ES cells (Wei et al., 2012; Zhang et al., 2013; Liang et al., 2010). Notably, Ying et al. found that the self-renewal of ES cells can be maintained at the ground state by inhibiting MAPK and GSK3 signaling pathways in the absence of the extracellular stimuli (Ying et al., 2008). Thus,

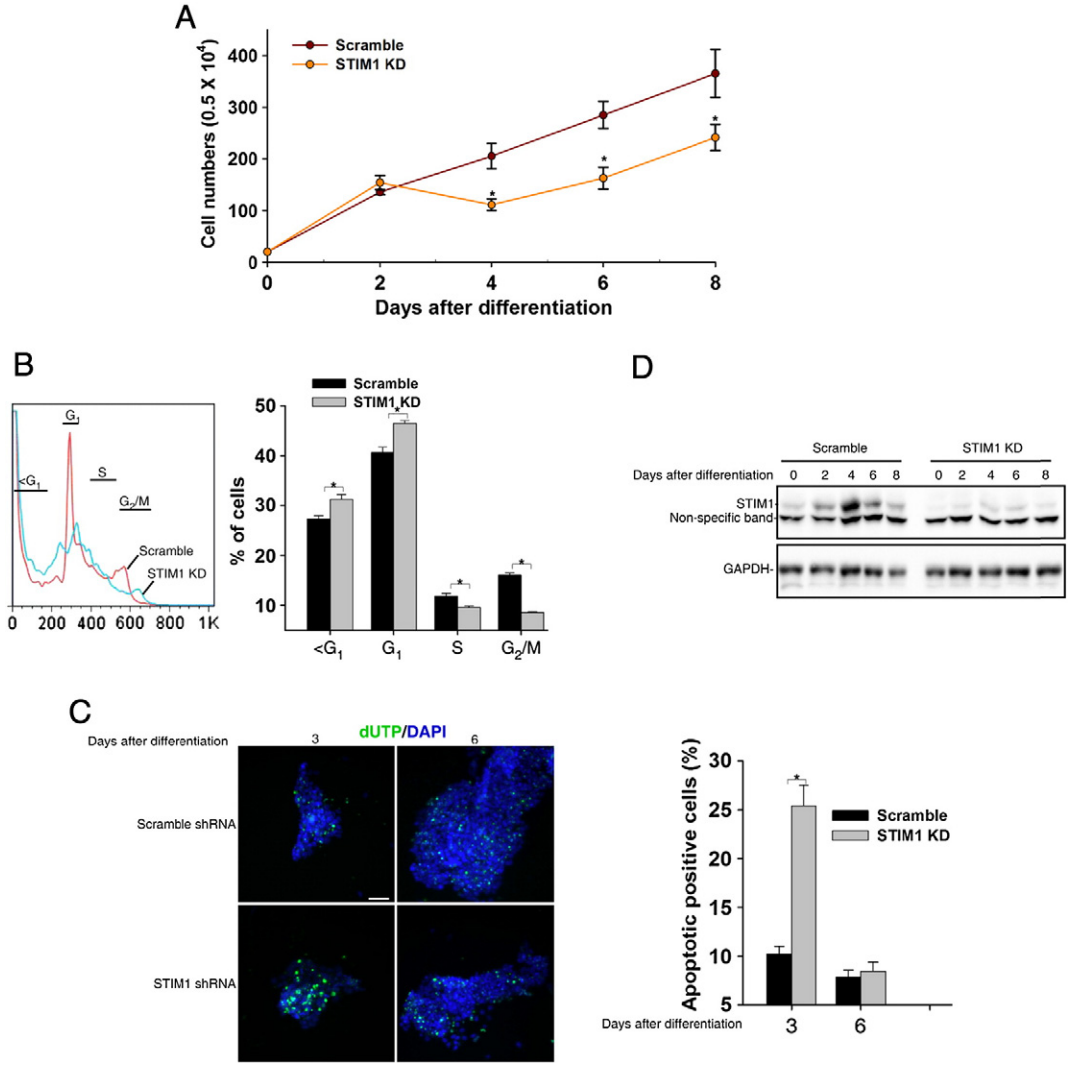

Figure 5 STIM1 knockdown markedly induced cell death during neural differentiation of mouse ES cells. (A) Live cell number counting of control and STIM1 knockdown 46C Sox1-GFP cells at indicated time points during neural differentiation. Data are expressed as mean ± S.E., n = 5. (B) FACS analyses of DNA contents (PI staining) in control and STIM1 knockdown 46C Sox1-GFP cells on day 4 after neural differentiation. Quantifications of the percentage of cells in each phase were expressed as mean ± S.E., n = 3. (C) TUNEL assays were performed in control and STIM1 knockdown D3 cells at indicated time point during neural differentiation (Scale bar = 50 μm). Data quantification was presented as TUNEL positive cells/DAPI-stained cells ± S.E., n = 5 (40–50 cells per experiment). The * symbols indicate the results of *t*-test analysis, $*p < 0.05$. (D) Cell lysates were harvested at indicated time points during neural differentiation in both control and STIM1 knockdown 46C Sox1-GFP cells, and analyzed for expression of STIM1 by western blot analyses.

ES cells might possess an innate program for the self-renewal without differentiation and are immune to the various extrinsic inputs.

The expressions of STIM1 and Orai1 were markedly increased during neural differentiation of mouse ES cells (Figs. 1C and D). In particular, the expression of STIM1 was peaked on day 4 after neural differentiation (Fig. 5D), suggesting that STIM1 may play an important role in the early stage of neural lineage entry. During the differentiation initiated by EB formation, expression of STIM1 or Orai1 was also markedly increased (Fig. S1). In addition, STIM1 expression showed a similar pattern during in vivo embryo development (Buchstaller et al., 2004). The increased expression of STIM1 and Orai1 during early development suggests that SOCE mediated by STIM1 and Orail1 is involved in multiple developmental processes, e.g. neurogenesis.

Indeed, we found STIM1 knockdown markedly inhibited both early and late neural differentiation of mouse ES cells. Sox1 is the specific marker of neuroectoderm, which was firstly detected in the neural plate of the embryo and was down-regulated during late neuronal and glial differentiation (Ying et al., 2003). By western blot and FACS analyses, we found that STIM1 knockdown decreased the expression of Sox1 during neural differentiation of ES cells (Fig. 4). In addition, the expressions of Tuj1 and GFAP, the marker for neurons and astrocytes, respectively, were decreased in the late neural differentiation of STIM1 knockdown ES cells compared to those in control cells (Fig. 6). These data

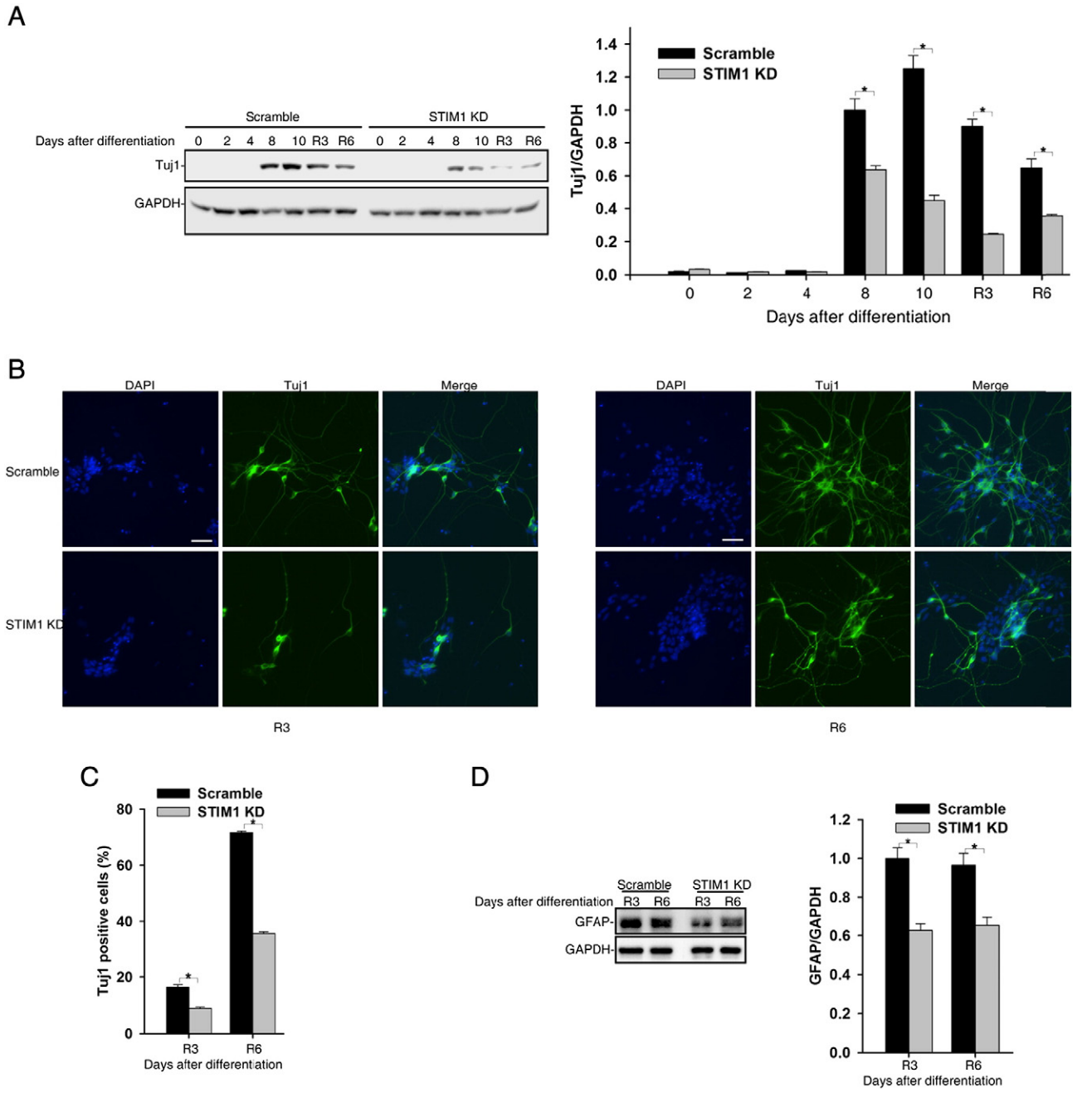

Figure 6 STIM1 knockdown inhibited terminal neural differentiation of 46C Sox1-GFP mouse ES cells. (A) Cell lysates were harvested at indicated time points during neural differentiation in both control and STIM1 knockdown cells, and analyzed for expression of Tuj1 by western blot analyses. (B) Immunofluorescent analysis of Tuj1 expression (Tuj1, Green; DAPI, blue) in control and STIM1 knockdown ES cells harvested at indicated time points during differentiation (Scale bar = 50 μm). (C) Data quantification of (B) was presented as Tuj1-positive cells/DAPI-stained cells ± S.E., n = 5 (40–50 cells per experiment), $*p < 0.05$. (D) Cell lysates were harvested at indicated time points during neural differentiation in both control and STIM1 knockdown cells, and analyzed for expression of GFAP by western blot analyses. R3 and R6 refer to day 3 and day 6, respectively, after replating differentiated cells to poly-L-lysine and laminin coated plates.

suggest that STIM1 is involved in both the early and late neural differentiation of mouse ES cells. Similarly, we also found that STIM2 knockdown markedly inhibited neural differentiation of mouse ES cells (Fig. S6). Moreover, STIM1 knockdown did not affect the expression of STIM2, and vice versa, suggesting that STIM1 and STIM2 are not functionally redundant (data not shown). Surprisingly, we found that Orai1 knockdown had little effect on neural differentiation (Fig. 7), yet STIM1 knockdown, STIM2 knockdown, and Orai1 knockdown all compromised SOCE in ES cell derived neurons (Figs. 8A, C, and S6B). Taken together, these data suggest that the inhibition of neural differentiation of mouse ES cells by STIM1 or STIM2 knockdown is independent of Orai1-mediated SOCE.

Actually, STIM1 has been shown to control several cellular processes independently of Orai1-mediated Ca^{2+} entry (Shinde et al., 2013). For example, two research groups have reported that STIM1 directly binds to VGCCs to inhibit their activity (Park et al., 2010; Wang et al., 2010b). The orchestration of these two Ca^{2+} signaling pathways by STIM1 may imply an important role in cellular activities of neurons. Here we found that STIM1 knockdown, not Orai1 knockdown, indeed enhanced the activity of VGCCs in ES cell derived neurons (Figs. 8B and D). Moreover, treatment of cells with nifedipine, a VGCC antagonist, facilitated the neural differentiation of both wildtype and STIM1 knockdown

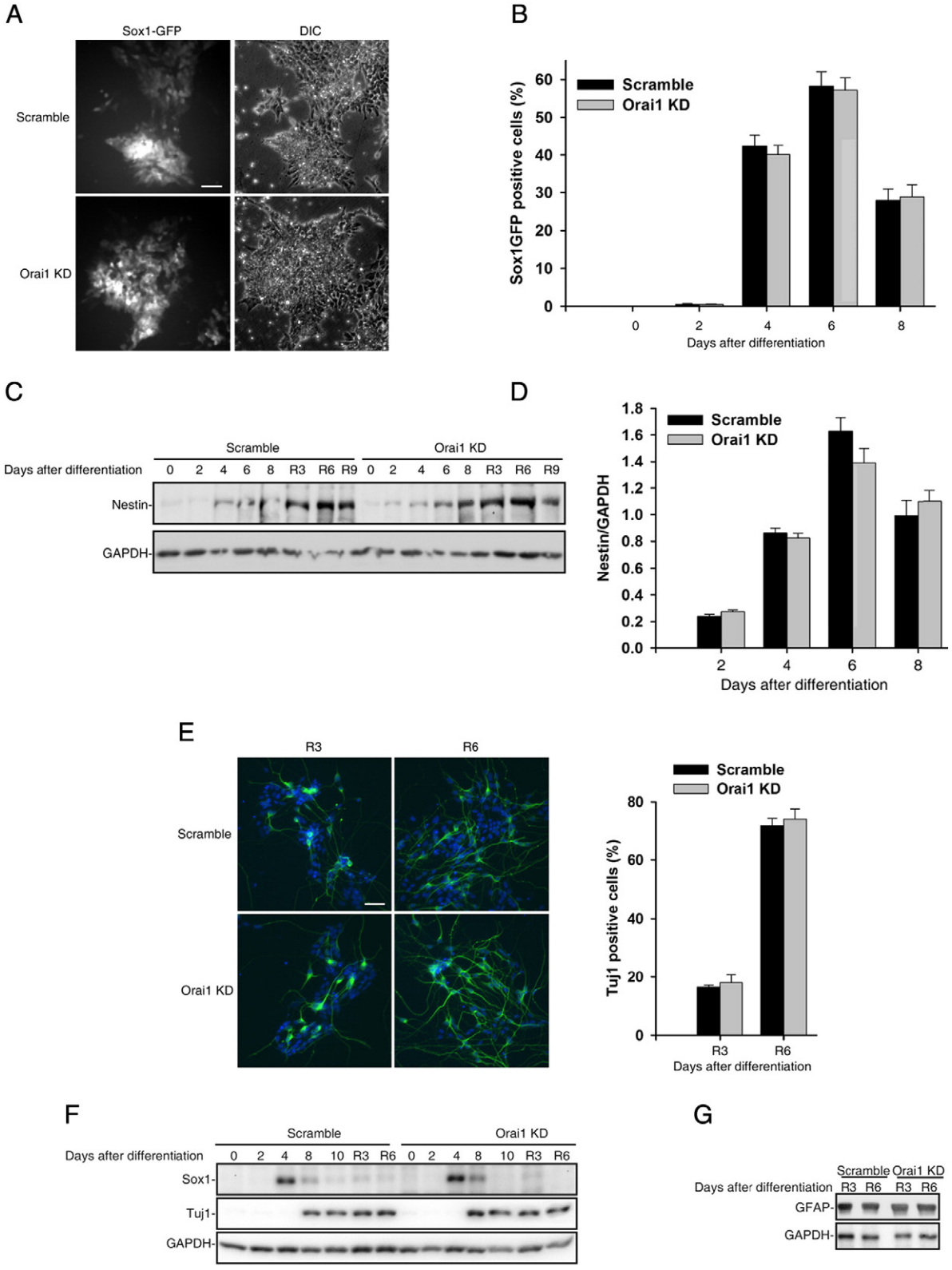

ES cells (Fig. S7). On the other hand, similar to STIM1 knockdown, treatment of cells with BayK 8644, a VGCC agonist, markedly decreased cell viability, and hardly any cells actually survived the late stage of neural differentiation (data not shown). These data suggest that STIM1 is required for neural differentiation of ES cells by suppressing VGCC activity. Interestingly, D'Ascenzo et al. found the opposite results when using nifedipine or BayK 8644 on mouse neural stem/progenitor cells (D'Ascenzo et al., 2006). Because it is well established that Ca^{2+} signaling temporally and spatially regulates early development, including neurogenesis, it is possible that VGCC plays differential roles in regulating early (from ES cells to neural progenitors) and late (from neural progenitors to terminal differentiated neurons) neural differentiation. Future studies will be performed to examine the interplay between STIM1 and VGCCs in the regulation of neural differentiation of mouse ES cells and whether VGCCs differentially regulate early and late neural differentiation.

Beside VGCCs, several studies showed that STIM1 directly binds and activates TRPCs for Ca^{2+} entry independent of Orai1 (Kim et al., 2009; Huang et al., 2006). Moreover, the TRPC1/STIM1/Ca^{2+} signaling pathway has been shown to play a role in neural development and neural related functions, including the proliferation of adult hippocampal neurogenesis, cell cycle distribution and fate determination of human neural progenitor cells (Morgan et al., 2013), and neurotransmitter regulation of salivary fluid secretion (Pani et al., 2013). Most recently, a TRPC1-mediated increase in store-operated Ca^{2+} entry was found to be required for the proliferation of adult hippocampal neural progenitor cells (M. Li et al., 2012). Whether the role of STIM1 in neural differentiation of ES cells is also related to TRPCs is of interest and needs to be determined.

Materials and methods

Cell culture

ES cell line 46C with GFP reporter knocked in *sox1* locus was a kind gift from Prof. Austin Smith, University of Cambridge (Ying et al., 2003). Undifferentiated ES cells were maintained in Dulbecco's Modified Eagle Medium (DMEM) with 15% ES qualified fetal bovine serum (FBS), 1% L-Glutamine, 1% penicllin–streptomcyin (P/S), 1% nonessential amino acids, 0.2% 2-mercaptoethanol, and 1000 units/ml leukemia inhibitory factor (LIF, Milipore) on 0.1% gelatin (Sigma-Aldrich) coated plates with feeder layer of mitotically inactivated mouse embryonic fibroblasts (mEFS). The cells were passaged every 2 days. Prior to any experimental procedure, ES cells were separated from feeder cells and cultured in standard ES medium on gelatin coated plates for 2 passages.

Neural differentiation

Undifferentiated feeder free ES cells were plated onto gelatin coated plates at a density of 0.8–1.3 × 10^4 cells/cm^2 in N2B27 medium (1:1 mixture of DMEM/F12 supplemented with N2 and 50 μg/ml bovine serum albumin (BSA) fraction V (Sigma-Aldrich) and neurobasal medium supplemented with B27 and 20 μM 2-mercaptoethanol). The medium was changed every 2 days until day 6. Neural entry normally starts after 3 or 4 days culture in N2B27 medium, which is termed as early neural differentiation. By day 6 after differentiation, majority of cells are neural progenitors. Thus, on day 6, cells were trypsinized and replated onto poly-L-lysine (25 μg/ml, Sigma-Aldrich) and laminin (10 μg/ml) coated plates at a density of 1.0–1.3 × 10^4 cells/cm^2 in N2B27 medium for late or terminal neuronal differentiation. The medium was changed every 3 or 4 days until 9 days after replating (Zhang et al., 2013).

EB formation

Undifferentiated ES cells were cultivated in a differentiation medium (standard ES medium without LIF) in hanging drops (800 cells/drop) for 2 days to form EBs, then kept in suspension culture for 3 days. Subsequently, EBs were plated onto gelatin coated plates for further differentiation. The medium was changed every 2 days. All cultivation medium and other substances were from Invitrogen–Gibco unless otherwise indicated.

STIM1 and Orai1 shRNA lentivirus production and infection

To construct STIM1 and Orai1 shRNA vectors, 2 pairs of independent oligo primers (Table S1) targeting STIM1 or Orai1, respectively, were subcloned into PLKO.1 vector (Addgene). Scramble shRNA vector was applied as control.

Figure 7 Orai1 knockdown had on effects on neural differentiation of 46C Sox1-GFP mouse ES cells. (A) GFP cell imaging and bright field of the Sox1-GFP positive cells in both control and Orai1 knockdown ES cells on day 4 after neural differentiation (Scale bar = 50 μm). (B) Quantification of FACS analyses of Sox1-GFP positive neural progenitors in control and Orai1 knockdown ES cells harvested at the indicated time point during neural differentiation. Data were expressed as mean ± S.E. n = 3. (C) Cell lysates were harvested at indicated time points during neural differentiation in both control and Orai1 knockdown cells, and analyzed for expression of Nestin by western blot analyses. (D) RNA was harvested at the indicated time points during neural differentiation of scramble shRNA infected and Orai1 knockdown ES cells and analyzed for expression of nestin by quantitative real-time RT-PCR. (E) Immunofluorescent analysis of Tuj1 expression (Tuj1, Green; DAPI, blue) in control and Orai1 knockdown ES cells harvested at indicated time points during differentiation (Scale bar = 50 μm). Data quantification was presented as Tuj1-positive cells/DAPI-stained cells ± S.E., n = 5 (40–50 cells per experiment). (F) Cell lysates were harvested at indicated time points during neural differentiation in both control and Orai1 knockdown cells, and analyzed for expression of Sox1 and Tuj1 by western blot analyses. (G) Cell lysates were harvested at indicated time points during neural differentiation in both control and Orai1 knockdown cells, and analyzed for expression of GFAP by western blot analyses. R3 and R6 refer to day 3 and day 6, respectively, after replating differentiated cells to poly-L-lysine and laminin coated plates.

Then lentivirus production was performed in HEK 293T cells. For infection, feeder free ES cells were plated at a density of 3×10^5 cells/well in 6-well plate. On the next day, lentiviruses of scramble shRNA, STIM1 shRNA, or Orai1 shRNA were added to cells in fresh medium containing 8 μg/ml polybrene. 36–48 h later, cells were selected in fresh medium with 3 μg/ml puromycin for 3–5 days. After selection, knockdown efficiencies were detected by western blot or *quantitive real-time* RT-PCR (qRT-PCR) analysis.

Western blot analysis

Briefly, cells were lyzed with ice-cold EBC lysis buffer (50 mM Tris–HCl pH 8.0, 120 mM NaCl, 0.5% Nonidet P-40, 100 mM NaF, 200 μM Na_3VO_4, 0.5% sodium deoxycholate, 0.1% SDS, 150 nM PMSF, 1 mM DTT, plus freshly added proteinase inhibitors of 10 μg/ml aprotinin, 1 μg/ml leupeptin, and 1 μg/ml pepstatin). Then cell lysate was passed through 21-gauge needles several times to disperse any large aggregates. Protein concentration was determined by Bradford protein assay (Bio-RAD). Proteins (30 μg protein per lane) were diluted with the standard SDS sample buffer and subjected to electrophoresis on 8 or 10% SDS polyacrylamide gels. The proteins were transferred to an Immobilon PVDF membrane (Millipore), blocked with 5% milk in TBST (20 mM Tris, 150 mM NaCl, pH 7.6, 0.1% Tween-20) for 1 h at room temperature, and incubated with the primary antibodies against STIM1 (610954, BD Biosciences, 1:1000 dilution), Oct4 (sc-8628, Santa Cruz, 1:1000 dilution), Nanog (ab80892, Abcam, 1:1000 dilution), Sox1 (MAB3369, R&D system, 1:1000 dilution), Nestin (#NES, Aves, 1:1000 dilution), Tuj1 (MAB1195, R&D system, 1:1000 dilution), GFAP (G9269, Sigma-Aldrich, 1:1000 dilution), or GAPDH (G8795, Sigma-Aldrich, 1:5000 dilution) overnight at 4 °C. After washing with TBST, the membranes were probed with HRP conjugated secondary antibodies for detection by chemiluminescence (Millipore).

RNA isolation and quantitative real-time RT-PCR

Total RNA of ES cells, neural differentiated cells, or EBs at specific time points were extracted with an RNA extraction kit (MACHEREY-NAGEL). The quantitative RT-PCR was performed with a MiniOpticonTM Real-time PCR Detection System (Bio-RAD) with a One-Step Q-RT PCR Kit (Takara) according to the manufacturer's instructions. The primers for detecting STIM1, Orai1, Nestin, and GAPDH were listed in supplemental Table S1. The relative gene expression was normalized to the expression of GAPDH.

Immunostaining analysis

Cells grown on coverslips at neuronal differentiation were fixed with 4% paraformaldehyde (PFA) for 20 min at room temperature, washed with PBS, and permeabilized with PBS containing 0.1% Triton X-100 (PBST) for 30 min. Thereafter, cells were blocked with 1% normal goat serum and 1% BSA in PBST for 1 h, and incubated with primary antibody Tuj1 (MRB4359, Covance, 1: 1000 dilution) for 2 h. After 3 wash with PBST, cells were incubated in secondary antibody (Alexa Fluor-488 goat anti-mouse IgG, A11008, Invitrogen, 1:500 dilution) for 1 h, followed by nuclei staining with DAPI (1:5000) for 2 min. Finally, cells were mounted with Prolong Gold Antifade Reagent (Invitrogen) on slides. Cells were visualized under an inverted Olympus IX81 fluorescence microscope with a CellR image system.

Alkaline phosphatase (AP) staining

AP staining was performed to determine the undifferentiated state of ES cells using an alkaline phosphatase detection kit (Millipore) according to the manufacturer's instruction. Briefly, ES Cells were fixed for 2 min at room temperature, and stained with mixture of Fast Red Violet solution with Naphthol AS-BI phosphate solution and water in a 2:1:1 ratio for 15 min in the dark at room temperature. Cells were washed with PBS and visualized under an Olympus inverted light microscope with a CCD camera.

Propidium iodide (PI) staining and flow cytometry analysis

Cells were plated in 6-well plates at a density of 2.5×10^5 cells/well and cultured for 2 days. Cells were fixed with 70% ethanol, and were then subjected to PI staining with 20 μg/ml PI, 0.1 mg/ml RNase A, 0.05% Triton X-100 in PBS for 10 min in the dark. Cells were filtered with a 40 μm cell stainer (BD Bioscience) and then analyzed by FACS Canto II analytic flow cytometer (BD Bioscience). Data were processed by FlowJo software.

Cell viability analysis

Cell viability was assessed by a 3-(4,5-dimethylthiazol-2-yl)-2,5-diphenyltetrazoliu-bromide (MTT) assay, a TUNEL assay, or simple cell counting technique. For the MTT assay, ES cells were plated onto 96-well plates at a density of 1000 cells/well and cultured for 4 days in the presence or absence of LIF. At the indicated times, 20 μl of MTT (5 mg/ml) was added and the cells were incubated for 4 h. Thereafter, cells were solubilized with DMSO and quantified in a plate reader at an absorbance of 570 nm.

For TUNEL assay, a DeadEnd™ Fluorometric TUNEL System (Promega) was applied. In brief, cells grown on coverslips were fixed with 4% PFA for 25 min at room temperature. The cells were then permeabilized with PBS plus 0.2% Triton X-100, equilibrated with equilibration buffer for 10 min at room temperature, and then incubated with TdT reaction mixture containing nucleotide mix and dTdT enzyme for 60 min at 37 °C in the dark. Fluorescein-12 dUTP was incorporated to the 3′-OH ends of fragmented DNA in apoptotic cells mediated by dTdT enzyme. The reaction was stopped with 2 × SSC buffer for 15 min at room temperature. Nuclei were stained with DAPI, and the coverslips were then mounted with Prolong Gold Antifade Reagent on slides. Cells were visualized with an Olympus inverted microscope.

The direct cell counting method was performed to determine the cell growth curve during neural differentiation. On differentiated days 2, 4, 6 and 8, cells were collected for cell counting and then stained with trypan blue to exclude the non-viable cells.

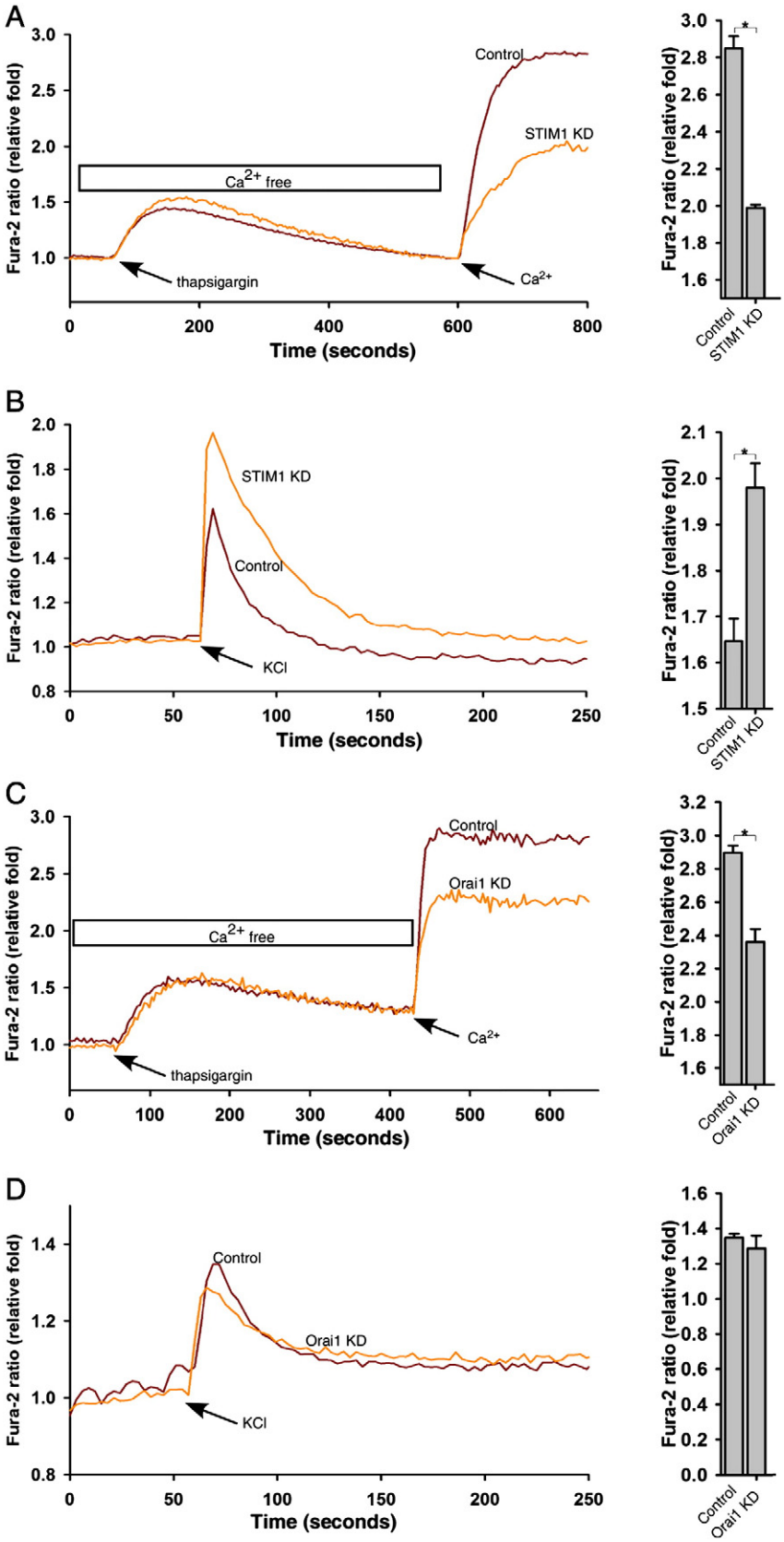

Figure 8 Ca^{2+} handling in neurons derived from control, STIM1 knockdown, and Orai1 knockdown mouse ES cells. (A) Thapsigargin (1 μM) induced-Ca^{2+} influx was inhibited by STIM1 knockdown in ES cell derived neurons. (B) KCl (30 mM) induced Ca^{2+} influx was enhanced by STIM1 knockdown in ES cell derived neurons. (C) Thapsigargin (1 μM) induced-Ca^{2+} influx was inhibited by Orai1 knockdown in ES cell derived neurons. (D) Orai1 knockdown had no effects on KCl (30 mM) induced Ca^{2+} influx in ES cell derived neurons. Quantifications of the peak of Ca^{2+} influx were expressed as mean ± S.E., n = 30–50 cells, $^*p < 0.05$.

Intracellular Ca^{2+} measurement

Cytosolic Ca^{2+} was measured as described previously (Yue et al., 2009; Lu et al., 2013). In brief, cells were plated onto 24-well plates at a density of 1×10^5 cells/well in regular medium for overnight and loaded with 4 μM Fura-2 AM in HBSS for 30 min at room temperature. Cells were then washed with HBSS 3 times and incubated at room temperature for another 15 min to de-esterify the dye. The cells were put on the stage of an Olympus inverted epifluorescence microscope and visualized using a 20× objective. Fluorescence images were obtained by alternate excitation at 340 nm and 380 nm with emission set at 510 nm. Images were collected by a CCD camera every 3 s and analyzed by a Cell R imaging software.

Statistical analysis

Data were presented as mean ± S.E.M. The statistical significance of differences was estimated by one-way ANOVA or Student's *t*-test. $p < 0.05$ was considered significant.

Acknowledgment

We thank Connie Lam and Yong-Juan Zhao for sharing reagents, and Richard Graeff and members of Yue lab for the advice on the manuscript. FACS analysis was performed in the Faculty of Medicine Core Facility at University of Hong Kong. This work was supported by the Research Grant Council (RGC) grants (HKU 782709M, HKU 785911M, HKU 769912M, and HKU 785213M) to J. Y.

Appendix A. Supplementary data

Supplementary data to this article can be found online at http://dx.doi.org/10.1016/j.scr.2013.12.005.

References

Abdelwahid, E., Siminiak, T., Guarita-Souza, L.C., Teixeira de Carvalho, K.A., Gallo, P., Shim, W., Condorelli, G., 2011. Stem cell therapy in heart diseases: a review of selected new perspectives, practical considerations and clinical applications. Curr. Cardiol. Rev. 7, 201–212.

Bain, G., Kitchens, D., Yao, M., Huettner, J.E., Gottlieb, D.I., 1995. Embryonic stem cells express neuronal properties in vitro. Dev. Biol. 168, 342–357.

Berridge, M.J., Bootman, M.D., Roderick, H.L., 2003. Calcium signalling: dynamics, homeostasis and remodelling. Nat. Rev. Mol. Cell Biol. 4, 517–529.

Braun, A., Varga-Szabo, D., Kleinschnitz, C., Pleines, I., Bender, M., Austinat, M., Bosl, M., Stoll, G., Nieswandt, B., 2009. Orai1 (CRACM1) is the platelet SOC channel and essential for pathological thrombus formation. Blood 113, 2056–2063.

Buchstaller, J., Sommer, L., Bodmer, M., Hoffmann, R., Suter, U., Mantei, N., 2004. Efficient isolation and gene expression profiling of small numbers of neural crest stem cells and developing Schwann cells. J. Neurosci. 24, 2357–2365.

Cajanek, L., Ribeiro, D., Liste, I., Parish, C.L., Bryja, V., Arenas, E., 2009. Wnt/beta-catenin signaling blockade promotes neuronal induction and dopaminergic differentiation in embryonic stem cells. Stem Cells 27, 2917–2927.

Chambers, I., Colby, D., Robertson, M., Nichols, J., Lee, S., Tweedie, S., Smith, A., 2003. Functional expression cloning of Nanog, a pluripotency sustaining factor in embryonic stem cells. Cell 113, 643–655.

Chhabra, P., Brayman, K.L., 2013. Stem cell therapy to cure type 1 diabetes: from hype to hope. Stem Cells Transl. Med. 2, 328–336.

Clapham, D.E., 2007. Calcium signaling. Cell 131, 1047–1058.

D'Ascenzo, M., Piacentini, R., Casalbore, P., Budoni, M., Pallini, R., Azzena, G.B., Grassi, C., 2006. Role of L-type Ca2+ channels in neural stem/progenitor cell differentiation. Eur. J. Neurosci. 23, 935–944.

Evans, M.J., Kaufman, M.H., 1981. Establishment in culture of pluripotential cells from mouse embryos. Nature 292, 154–156.

Feng, M., Grice, D.M., Faddy, H.M., Nguyen, N., Leitch, S., Wang, Y., Muend, S., Kenny, P.A., Sukumar, S., Roberts-Thomson, S.J., Monteith, G.R., Rao, R., 2010. Store-independent activation of Orai1 by SPCA2 in mammary tumors. Cell 143, 84–98.

Feske, S., Gwack, Y., Prakriya, M., Srikanth, S., Puppel, S.H., Tanasa, B., Hogan, P.G., Lewis, R.S., Daly, M., Rao, A., 2006. A mutation in Orai1 causes immune deficiency by abrogating CRAC channel function. Nature 441, 179–185.

Gaspard, N., Vanderhaeghen, P., 2010. Mechanisms of neural specification from embryonic stem cells. Curr. Opin. Neurobiol. 20, 37–43.

Gemes, G., Bangaru, M.L., Wu, H.E., Tang, Q., Weihrauch, D., Koopmeiners, A.S., Cruikshank, J.M., Kwok, W.M., Hogan, Q.H., 2011. Store-operated Ca2+ entry in sensory neurons: functional role and the effect of painful nerve injury. J. Neurosci. 31, 3536–3549.

Gruszczynska-Biegala, J., Pomorski, P., Wisniewska, M.B., Kuznicki, J., 2011. Differential roles for STIM1 and STIM2 in store-operated calcium entry in rat neurons. PLoS One 6, e19285.

Gwack, Y., Srikanth, S., Oh-Hora, M., Hogan, P.G., Lamperti, E.D., Yamashita, M., Gelinas, C., Neems, D.S., Sasaki, Y., Feske, S., Prakriya, M., Rajewsky, K., Rao, A., 2008. Hair loss and defective T- and B-cell function in mice lacking ORAI1. Mol. Cell. Biol. 28, 5209–5222.

Hawkins, B.J., Irrinki, K.M., Mallilankaraman, K., Lien, Y.C., Wang, Y., Bhanumathy, C.D., Subbiah, R., Ritchie, M.F., Soboloff, J., Baba, Y., Kurosaki, T., Joseph, S.K., Gill, D.L., Madesh, M., 2010. S-glutathionylation activates STIM1 and alters mitochondrial homeostasis. J. Cell Biol. 190, 391–405.

Huang, G.N., Zeng, W., Kim, J.Y., Yuan, J.P., Han, L., Muallem, S., Worley, P.F., 2006. STIM1 carboxyl-terminus activates native SOC, I(crac) and TRPC1 channels. Nat. Cell Biol. 8, 1003–1010.

Hulot, J.S., Fauconnier, J., Ramanujam, D., Chaanine, A., Aubart, F., Sassi, Y., Merkle, S., Cazorla, O., Ouille, A., Dupuis, M., Hadri, L., Jeong, D., Muhlstedt, S., Schmitt, J., Braun, A., Benard, L., Saliba, Y., Laggerbauer, B., Nieswandt, B., Lacampagne, A., Hajjar, R.J., Lompre, A.M., Engelhardt, S., 2011. Critical role for stromal interaction molecule 1 in cardiac hypertrophy. Circulation 124, 796–805.

Kawasaki, H., Mizuseki, K., Nishikawa, S., Kaneko, S., Kuwana, Y., Nakanishi, S., Nishikawa, S.I., Sasai, Y., 2000. Induction of midbrain dopaminergic neurons from ES cells by stromal cell-derived inducing activity. Neuron 28, 31–40.

Kim, J.H., Auerbach, J.M., Rodriguez-Gomez, J.A., Velasco, I., Gavin, D., Lumelsky, N., Lee, S.H., Nguyen, J., Sanchez-Pernaute, R., Bankiewicz, K., McKay, R., 2002. Dopamine neurons derived from embryonic stem cells function in an animal model of Parkinson's disease. Nature 418, 50–56.

Kim, M.S., Zeng, W., Yuan, J.P., Shin, D.M., Worley, P.F., Muallem, S., 2009. Native store-operated Ca2+ influx requires the channel function of Orai1 and TRPC1. J. Biol. Chem. 284, 9733–9741.

Koss, D.J., Riedel, G., Bence, K., Platt, B., 2013. Store-operated Ca2+ entry in hippocampal neurons: regulation by protein tyrosine phosphatase PTP1B. Cell Calcium 53, 125–138.

Kriks, S., Shim, J.W., Piao, J., Ganat, Y.M., Wakeman, D.R., Xie, Z., Carrillo-Reid, L., Auyeung, G., Antonacci, C., Buch, A., Yang, L., Beal, M.F., Surmeier, D.J., Kordower, J.H., Tabar, V., Studer,

L., 2011. Dopamine neurons derived from human ES cells efficiently engraft in animal models of Parkinson's disease. Nature 480, 547–551.
Li, D., Herault, K., Oheim, M., Ropert, N., 2009. FM dyes enter via a store-operated calcium channel and modify calcium signaling of cultured astrocytes. Proc. Natl. Acad. Sci. U. S. A. 106, 21960–21965.
Li, S., Hao, B., Lu, Y., Yu, P., Lee, H.C., Yue, J., 2012. Intracellular alkalinization induces cytosolic Ca2+ increases by inhibiting sarco/endoplasmic reticulum Ca2+–ATPase (SERCA). PLoS One 7, e31905.
Li, M., Chen, C., Zhou, Z., Xu, S., Yu, Z., 2012. A TRPC1-mediated increase in store-operated Ca2+ entry is required for the proliferation of adult hippocampal neural progenitor cells. Cell Calcium 51, 486–496.
Liang, J., Wang, Y.J., Tang, Y., Cao, N., Wang, J., Yang, H.T., 2010. Type 3 inositol 1,4,5-trisphosphate receptor negatively regulates apoptosis during mouse embryonic stem cell differentiation. Cell Death Differ. 17, 1141–1154.
Lindvall, O., 2012. Dopaminergic neurons for Parkinson's therapy. Nat. Biotechnol. 30, 56–58.
Lippmann, E.S., Azarin, S.M., Kay, J.E., Nessler, R.A., Wilson, H.K., Al-Ahmad, A., Palecek, S.P., Shusta, E.V., 2012. Derivation of blood–brain barrier endothelial cells from human pluripotent stem cells. Nat. Biotechnol. 30, 783–791.
Loh, Y.H., Wu, Q., Chew, J.L., Vega, V.B., Zhang, W., Chen, X., Bourque, G., George, J., Leong, B., Liu, J., Wong, K.Y., Sung, K.W., Lee, C.W., Zhao, X.D., Chiu, K.P., Lipovich, L., Kuznetsov, V.A., Robson, P., Stanton, L.W., Wei, C.L., Ruan, Y., Lim, B., Ng, H.H., 2006. The Oct4 and Nanog transcription network regulates pluripotency in mouse embryonic stem cells. Nat. Genet. 38, 431–440.
Lu, Y., Hao, B.X., Graeff, R., Wong, C.W., Wu, W.T., Yue, J., 2013. Two pore channel 2 (TPC2) inhibits autophagosomal–lysosomal fusion by alkalinizing lysosomal pH. J. Biol. Chem. 288, 24247–24263.
Mancarella, S., Wang, Y., Deng, X., Landesberg, G., Scalia, R., Panettieri, R.A., Mallilankaraman, K., Tang, X.D., Madesh, M., Gill, D.L., 2011. Hypoxia-induced acidosis uncouples the STIM-Orai calcium signaling complex. J. Biol. Chem. 286, 44788–44798.
Mitchell, C.B., Gasperini, R.J., Small, D.H., Foa, L., 2012. STIM1 is necessary for store-operated calcium entry in turning growth cones. J. Neurochem. 122, 1155–1166.
Moreno, C., Sampieri, A., Vivas, O., Pena-Segura, C., Vaca, L., 2012. STIM1 and Orai1 mediate thrombin-induced Ca(2+) influx in rat cortical astrocytes. Cell Calcium 52, 457–467.
Morgan, P.J., Hubner, R., Rolfs, A., Frech, M.J., 2013. Spontaneous calcium transients in human neural progenitor cells mediated by transient receptor potential channels. Stem Cells Dev. 22, 2477–2486.
Nichols, J., Zevnik, B., Anastassiadis, K., Niwa, H., Klewe-Nebenius, D., Chambers, I., Scholer, H., Smith, A., 1998. Formation of pluripotent stem cells in the mammalian embryo depends on the POU transcription factor Oct4. Cell 95, 379–391.
Oh-Hora, M., Yamashita, M., Hogan, P.G., Sharma, S., Lamperti, E., Chung, W., Prakriya, M., Feske, S., Rao, A., 2008. Dual functions for the endoplasmic reticulum calcium sensors STIM1 and STIM2 in T cell activation and tolerance. Nat. Immunol. 9, 432–443.
Pani, B., Liu, X., Bollimuntha, S., Cheng, K.T., Niesman, I.R., Zheng, C., Achen, V.R., Patel, H.H., Ambudkar, I.S., Singh, B.B., 2013. Impairment of TRPC1-STIM1 channel assembly and AQP5 translocation compromise agonist-stimulated fluid secretion in mice lacking caveolin1. J. Cell Sci. 126, 667–675.
Parekh, A.B., Putney Jr., J.W., 2005. Store-operated calcium channels. Physiol. Rev. 85, 757–810.
Park, C.Y., Shcheglovitov, A., Dolmetsch, R., 2010. The CRAC channel activator STIM1 binds and inhibits L-type voltage-gated calcium channels. Science 330, 101–105.
Picard, C., McCarl, C.A., Papolos, A., Khalil, S., Luthy, K., Hivroz, C., LeDeist, F., Rieux-Laucat, F., Rechavi, G., Rao, A., Fischer, A., Feske, S., 2009. STIM1 mutation associated with a syndrome of immunodeficiency and autoimmunity. N. Engl. J. Med. 360, 1971–1980.
Riccardi, C., Nicoletti, I., 2006. Analysis of apoptosis by propidium iodide staining and flow cytometry. Nat. Protoc. 1, 1458–1461.
Shinde, A.V., Motiani, R.K., Zhang, X., Abdullaev, I.F., Adam, A.P., Gonzalez-Cobos, J.C., Zhang, W., Matrougui, K., Vincent, P.A., Trebak, M., 2013. STIM1 controls endothelial barrier function independently of Orai1 and Ca2+ entry. Sci. Signal. 6, ra18.
Steinbeck, J.A., Henke, N., Opatz, J., Gruszczynska-Biegala, J., Schneider, L., Theiss, S., Hamacher, N., Steinfarz, B., Golz, S., Brustle, O., Kuznicki, J., Methner, A., 2011. Store-operated calcium entry modulates neuronal network activity in a model of chronic epilepsy. Exp. Neurol. 232, 185–194.
Stiber, J., Hawkins, A., Zhang, Z.S., Wang, S., Burch, J., Graham, V., Ward, C.C., Seth, M., Finch, E., Malouf, N., Williams, R.S., Eu, J.P., Rosenberg, P., 2008. STIM1 signalling controls store-operated calcium entry required for development and contractile function in skeletal muscle. Nat. Cell Biol. 10, 688–697.
Tian, L.P., Zhang, S., Xu, L., Li, W., Wang, Y., Chen, S.D., Ding, J.Q., 2012. Selenite benefits embryonic stem cells therapy in Parkinson's disease. Curr. Mol. Med. 12, 1005–1014.
Tropepe, V., Hitoshi, S., Sirard, C., Mak, T.W., Rossant, J., van der Kooy, D., 2001. Direct neural fate specification from embryonic stem cells: a primitive mammalian neural stem cell stage acquired through a default mechanism. Neuron 30, 65–78.
Venkiteswaran, G., Hasan, G., 2009. Intracellular Ca2+ signaling and store-operated Ca2+ entry are required in Drosophila neurons for flight. Proc. Natl. Acad. Sci. U. S. A. 106, 10326–10331.
Vig, M., Peinelt, C., Beck, A., Koomoa, D.L., Rabah, D., Koblan-Huberson, M., Kraft, S., Turner, H., Fleig, A., Penner, R., Kinet, J.P., 2006a. CRACM1 is a plasma membrane protein essential for store-operated Ca2+ entry. Science 312, 1220–1223.
Vig, M., Beck, A., Billingsley, J.M., Lis, A., Parvez, S., Peinelt, C., Koomoa, D.L., Soboloff, J., Gill, D.L., Fleig, A., Kinet, J.P., Penner, R., 2006b. CRACM1 multimers form the ion-selective pore of the CRAC channel. Curr. Biol. 16, 2073–2079.
Wang, Y., Deng, X., Gill, D.L., 2010a. Calcium signaling by STIM and Orai: intimate coupling details revealed. Sci. Signal. 3, pe42.
Wang, Y., Deng, X., Mancarella, S., Hendron, E., Eguchi, S., Soboloff, J., Tang, X.D., Gill, D.L., 2010b. The calcium store sensor, STIM1, reciprocally controls Orai and CaV1.2 channels. Science 330, 105–109.
Wei, W.J., Sun, H.Y., Ting, K.Y., Zhang, L.H., Lee, H.C., Li, G.R., Yue, J., 2012. Inhibition of cardiomyocytes differentiation of mouse embryonic stem cells by CD38/cADPR/Ca2+ signaling pathway. J. Biol. Chem. 287, 35599–35611.
Wiles, M.V., Johansson, B.M., 1999. Embryonic stem cell development in a chemically defined medium. Exp. Cell Res. 247, 241–248.
Xiao, B., Coste, B., Mathur, J., Patapoutian, A., 2011. Temperature-dependent STIM1 activation induces Ca(2)+ influx and modulates gene expression. Nat. Chem. Biol. 7, 351–358.
Ying, Q.L., Smith, A.G., 2003. Defined conditions for neural commitment and differentiation. Methods Enzymol. 365, 327–341.
Ying, Q.L., Stavridis, M., Griffiths, D., Li, M., Smith, A., 2003. Conversion of embryonic stem cells into neuroectodermal precursors in adherent monoculture. Nat. Biotechnol. 21, 183–186.
Ying, Q.L., Wray, J., Nichols, J., Batlle-Morera, L., Doble, B., Woodgett, J., Cohen, P., Smith, A., 2008. The ground state of embryonic stem cell self-renewal. Nature 453, 519–523.
Yue, J., Wei, W., Lam, C.M., Zhao, Y.J., Dong, M., Zhang, L.R., Zhang, L.H., Lee, H.C., 2009. CD38/cADPR/Ca2+ pathway promotes cell proliferation and delays nerve growth factor-induced differentiation in PC12 cells. J. Biol. Chem. 284, 29335–29342.

Zhang, S.L., Yu, Y., Roos, J., Kozak, J.A., Deerinck, T.J., Ellisman, M.H., Stauderman, K.A., Cahalan, M.D., 2005. STIM1 is a Ca2+ sensor that activates CRAC channels and migrates from the Ca2+ store to the plasma membrane. Nature 437, 902–905.

Zhang, W., Halligan, K.E., Zhang, X., Bisaillon, J.M., Gonzalez-Cobos, J.C., Motiani, R.K., Hu, G., Vincent, P.A., Zhou, J., Barroso, M., Singer, H.A., Matrougui, K., Trebak, M., 2011. Orai1-mediated I (CRAC) is essential for neointima formation after vascular injury. Circ. Res. 109, 534–542.

Zhang, Z.-H., Lu, Y.-Y., Yue, J., 2013. Two pore channel 2 differentially modulates neural differentiation of mouse embryonic stem cells. PLoS One 8, e66077.